

Orientation and Morphology Control in Acid-Catalyzed Covalent Organic Framework Thin Films

Dayanni D. Bhagwandin,^{a,b} Kirt A. Page,^{a,b,c} Ly D. Tran,^{a,b} Yao Yao,^d Alexander Reidell,^{a,b} Christopher Muratore^e Qiyi Fang,^{f,g} Aleksey Ruditskiy,^{a,b} Cheri M. Hampton,^{a,b} W. Joshua Kennedy,^a Lawrence F. Drummy,^a Yu Zhong,^g Tobin J. Marks,^d Antonio Facchetti,^{d,h} Jun Lou,^f Hilmar Koerner,^a Luke A. Baldwin,^a Nicholas R. Glavin^{†a}

-
- ^a. *Materials and Manufacturing Directorate, Air Force Research Laboratory, Wright-Patterson Air Force Base, Ohio 45433, USA*
- ^b. *UES, Inc., Beavercreek, Ohio 45432, USA*
- ^c. *Cornell High Energy Synchrotron Source, Cornell University, Ithaca, New York 14853, USA*
- ^d. *Department of Chemistry and the Materials Research Center, Northwestern University, Sheridan Road, Evanston, IL 60208 USA*
- ^e. *Department of Chemical and Materials Engineering, University of Dayton, Dayton, Ohio 45469, USA*
- ^f. *Department of Materials Science and NanoEngineering, Rice University, Houston, Texas 77005, USA*
- ^g. *Department of Materials Science and Engineering, Cornell University, Ithaca, New York 14853, United States*
- ^h. *School of Materials Science and Engineering, Georgia Institute of Technology, Atlanta, Georgia 30332, USA*

Table of Contents

I. General Information	4
Reagents.....	4
Data.....	4
Raman Spectroscopy	4
Fourier Transform-Infrared Spectroscopy (FT-IR)	4
UV-Vis Absorption Spectroscopy	4
Transmission Electron Microscopy (TEM).....	4
Scanning Electron Microscopy (SEM).....	4
Grazing-Incidence Wide-Angle X-Ray Scattering (GIWAXS)	4
Powder X-Ray Diffraction (PXRD)	5
II. COF Synthesis.....	5
III. Liquid–Liquid (LL) TAPB-PDA COF Characterization	6
Powder X-Ray Diffraction TAPB-PDA COF (LL).....	6
FT-IR Spectroscopy of TAPB-PDA COF (LL) versus Starting Materials.....	7
IV. Liquid–Solid (LS) TAPB-PDA COF Characterization.....	8
Energy Dispersive X-Ray Spectroscopy (EDX) of TAPB-PDA COF (LS).....	8
Transmission Electron Microscopy of TAPB-PDA COF (LS)	10
Raman Spectroscopy of TAPB-PDA COF (LS) at Different Acid Concentrations	12
Time-lapse of Interfacial COF Growth Setup	13
Film Morphology of TAPB-PDA COF (LS).....	14
Early Growth Experiment of TAPB-PDA COF (LS).....	15
X-Ray Comparison of LL and LS TAPB-PDA COFs.....	23
Lattice Constant Calculation of LS and LL TAPB-PDA COF from GIWAXS.....	24
V. Device Information.....	25
Fabrication	25
Transistor Measurement	26
VI. References	27

I. General Information

Reagents

All reagents were purchased from commercial suppliers. 1,3,5-tris(4-aminophenyl)benzene (TAPB) was purchased from Ambeed, Inc. with a 97% purity. 1,4-terephthalaldehyde (PDA) was purchased from Aldrich with a 99% purity.

Data

All data was plotted using Origin Pro.

Raman Spectroscopy

Raman spectra were collected using 514 nm excitation wavelength in a Renishaw inVia Raman microscope. A 50 x objective lens was used to focus the incident laser beam on the samples and the laser power was set to 0.5 mW. Raman spectra were collected from the samples with 40 second acquisition times and 1 acquisition.

Fourier Transform-Infrared Spectroscopy (FT-IR)

Data was collected using a Bruker Invenio X FT-IR in ATR mode on solid powders of the materials. The scanner rate was 10 kHz.

UV-Vis Absorption Spectroscopy

Data was collected using an Agilent Cary 5000 UV-Vis-NIR.

Transmission Electron Microscopy (TEM)

Prepared tem grids were imaged on a Thermo Fisher Scientific Talos 200C at magnifications of 120-310kx. Projection images were recorded on a 4K Ceta CCD camera.

Scanning Electron Microscopy (SEM)

Characterization was performed using an Apreo 2 (Thermo Fisher Scientific, Waltham, Massachusetts, USA) at ~3.50 and ~10.0 kV. The samples were coated with ~5nm of AuPd alloy prior to imaging in order to reduce surface charging and improve picture quality.

Grazing-Incidence Wide-Angle X-Ray Scattering (GIWAXS)

The grazing-incidence X-ray scattering measurements were carried out at the Functional Materials Beamline (FMB) of the Materials Solutions Network at the Cornell High Energy Synchrotron Source (MSN-CHESS). An X-ray beam energy of 9.7 keV ($\lambda=1.28 \text{ \AA}$) was selected using the 111 reflection of a single-bounce, HPHT diamond monochromator.¹ Harmonic rejection and vertical focusing are provided by a 1-meter long, bendable, rhodium-coated monochromatic mirror located approximately 7 meters upstream of the experimental hutch at an incident angle of 4 milliradians. Experiments were carried out in “bulk-beam” mode and the monochromatic mirror was used to focus the beam into a spot approximately 0.045 x 0.5 mm² at

the sample position, with a total flux of approximately 10^{12} photons/secondⁱ at 100 mA beam current. The samples were mounted on a 4-axis goniometer and aligned using a downstream ion chamber. Experiments were performed over a range of incident angles, both below and above the film critical angle. Scattering images were collected on a Pilatus 300K detector (Dectris, Baden, Switzerland) with a sample-to-detector distance of ca. 81.6 cm. Detector images were calibrated using silver behenate to convert the images to q-space. ImageJ software² was used to analyze the scattering images and to produce intensity versus scattering vector, $q(\text{\AA}^{-1})$, plots.

Powder X-Ray Diffraction (PXRD)

Data was collected on a Rigaku Smartlab diffractometer with a $\text{CuK}\alpha(1.5406 \text{ \AA})$ X-ray radiation source and was operated at 40 V and 44 mA. The scan speed was $2.0^\circ/\text{min}$.

II. COF Synthesis

1,3,5-tris(4-aminophenyl) benzene (TAPB) (13 mg, 0.04 mmol, 1.0 eq) and *p*-phthalaldehyde (PDA) (7.5 mg, 0.06 mmol, 1.5 eq), which were added to a 20 mL scintillation vial and mixed with methylene chloride (8 mL). The mixture was then sonicated for 5 minutes to ensure the precursors were fully dissolved. Then 8 mL of aqueous acetic acid (from 1 M to 10 M) was slowly syringed on top of the organic layer.

The liquid-liquid film analysed with GIWAXS was synthesized over 3 days in a petri dish using 0.1 M acetic acid as the bottom layer and mesitylene as the top layer

Prior to GIWAXS studies, all films were subjected to an annealing step using a modified procedure.³ Films were saturated with a dioxane, mesitylene, and 10 M acetic acid (6.7:1.7:1, v/v) solution. Then they were placed in a chamber above the same solvent and subjected to the vapors by heating at 70°C for 2 hours. Following this the films were activated under nitrogen flow by heated to 150°C (50 degree intervals, 30 minutes each). AFM analysis reveals so significant change in film morphology before and after these steps.

III. Liquid–Liquid (LL) TAPB-PDA COF Characterization

Structural and chemical characterization of the TAPB-PDA COF (LL) carried out using powder X-ray diffraction (PXRD), Fourier-transform infrared spectroscopy (FT-IR), Raman spectroscopy, and Grazing-Incidence Wide-Angle X-Ray Scattering (GIWAXS).

Powder X-Ray Diffraction TAPB-PDA COF (LL)

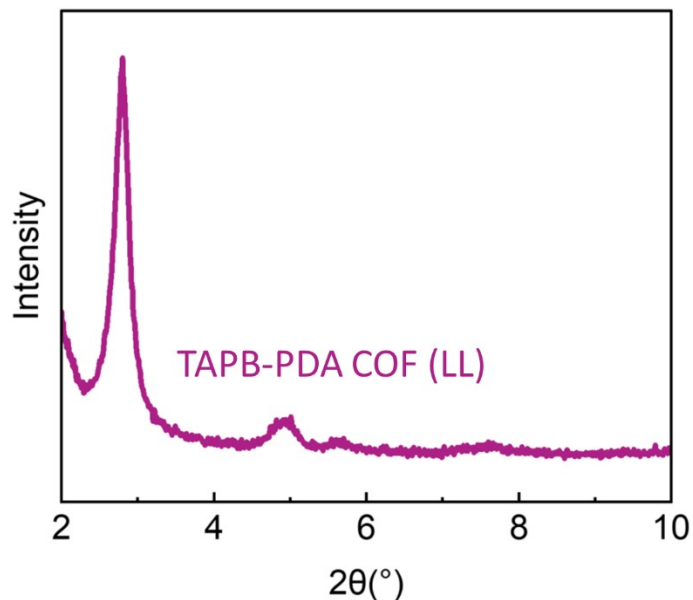


Figure S1. Powder X-Ray Diffraction (PXRD) of TAPB-PDA COF grown at liquid–liquid interface.

PXRD of the solid COF (LL) film grown after 24 hours analysis shows peaks at 2.8, 4.7, 5.6, and 7.4 2θ corresponding to the $\langle 100 \rangle$, $\langle 110 \rangle$, $\langle 200 \rangle$, and $\langle 210 \rangle$ planes, respectively.

FT-IR Spectroscopy of TAPB-PDA COF (LL) versus Starting Materials

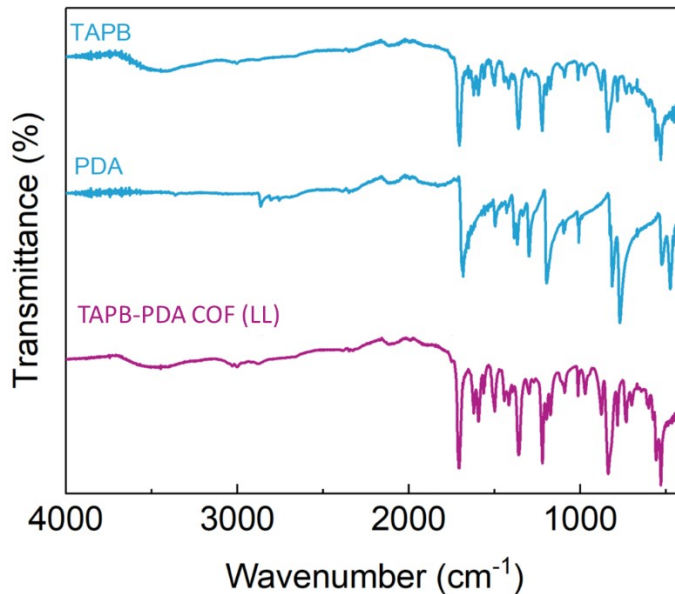


Figure S2. Fourier-Transform Infrared Spectroscopy of starting materials (TAPB and PDA) and TAPB-PDA COF (LL).

FT-IR spectroscopy of the same material revealed the absence of starting material, as indicated by the missing C=O (1,690 cm⁻¹) and N-H (3,350 cm⁻¹) stretching bands in PDA and TAPB, respectively. A peak at 1,700 cm⁻¹ was observed which corresponds to the stretching bands from the C=N in the newly formed imine bond.

Raman spectroscopy of the same material showed the absence of starting material peaks and the presence of peaks at 1,590, 1,560, and 1,160 cm⁻¹ corresponding to a previous literature report for TAPB-PDA COF.⁴ This is depicted in the main manuscript text.

IV. Liquid–Solid (LS) TAPB-PDA COF Characterization

Chemical characterization of the TAPB-PDA COF (LS) was carried out using Raman spectroscopy and Energy dispersive X-Ray spectroscopy (EDX). The Raman spectroscopy can be found in the main manuscript text as well as in Figure S7. Raman spectroscopy of the films showed the exact same pattern of the characterized TAPB-PDA (LL) COF, with the exception of a peak at 520 cm^{-1} which corresponds to the SiO_2/Si substrate.

Energy Dispersive X-Ray Spectroscopy (EDX) of TAPB-PDA COF (LS)

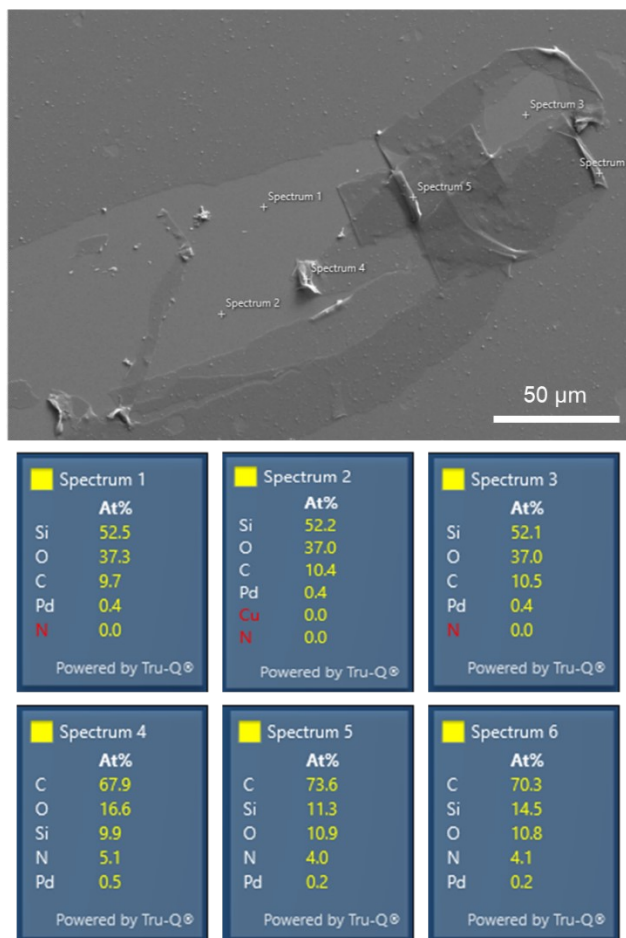


Figure S3. EDX Analysis of TAPB-PDA COF Film (LS) (2 M, 24 hour growth); substrate corresponds to spectrums 1-3, COF corresponds to spectrums 5-6.

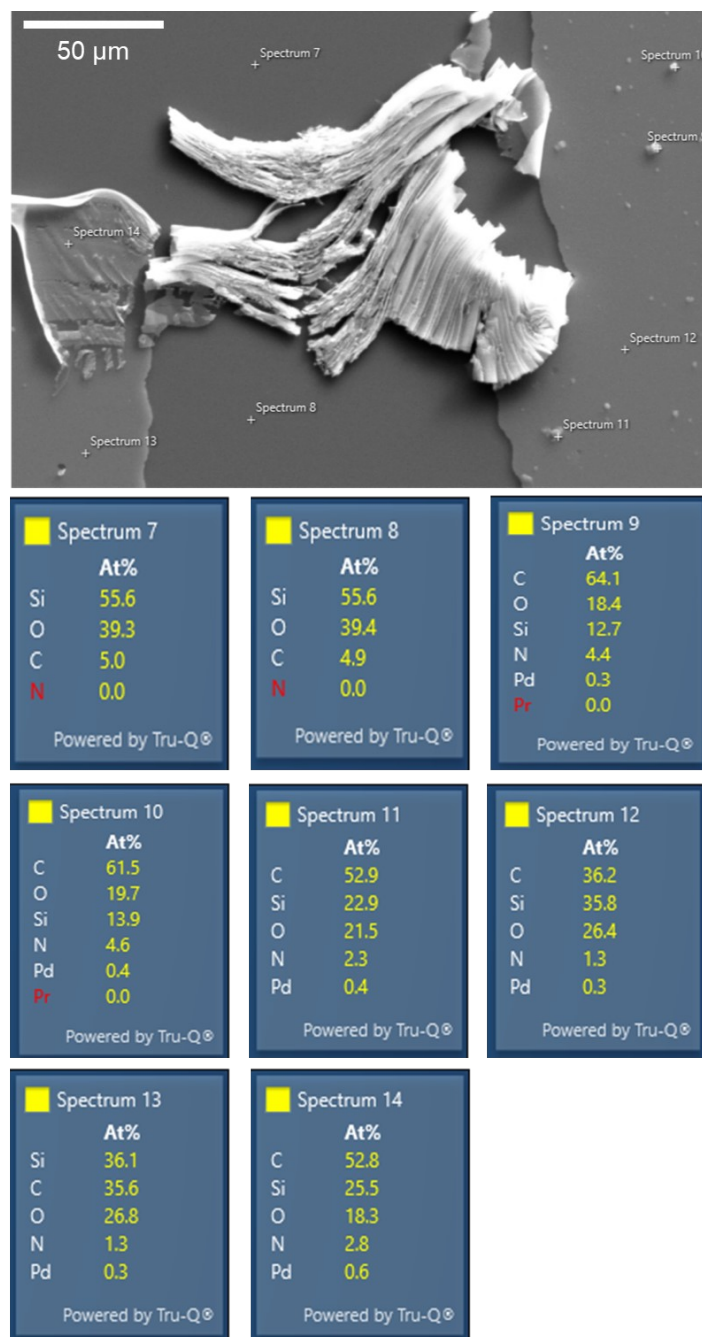


Figure S4. EDX Analysis of TAPB-PDA COF Film (LS) (2 M, 24 hour growth); substrate corresponds to spectrums 7 and 8, COF corresponds to spectrums 9-14.

EDX analysis of areas of the film show around 30-70% carbon and 1-5% nitrogen where areas of substrate show mainly silicon.

Structural characterization of the TAPB-PDA COF (LS) was carried out using GIWAXS and Transmission Electron Microscopy (TEM) which are shown in the main manuscript and in Figures S5 and S6.

Transmission Electron Microscopy of TAPB-PDA COF (LS)

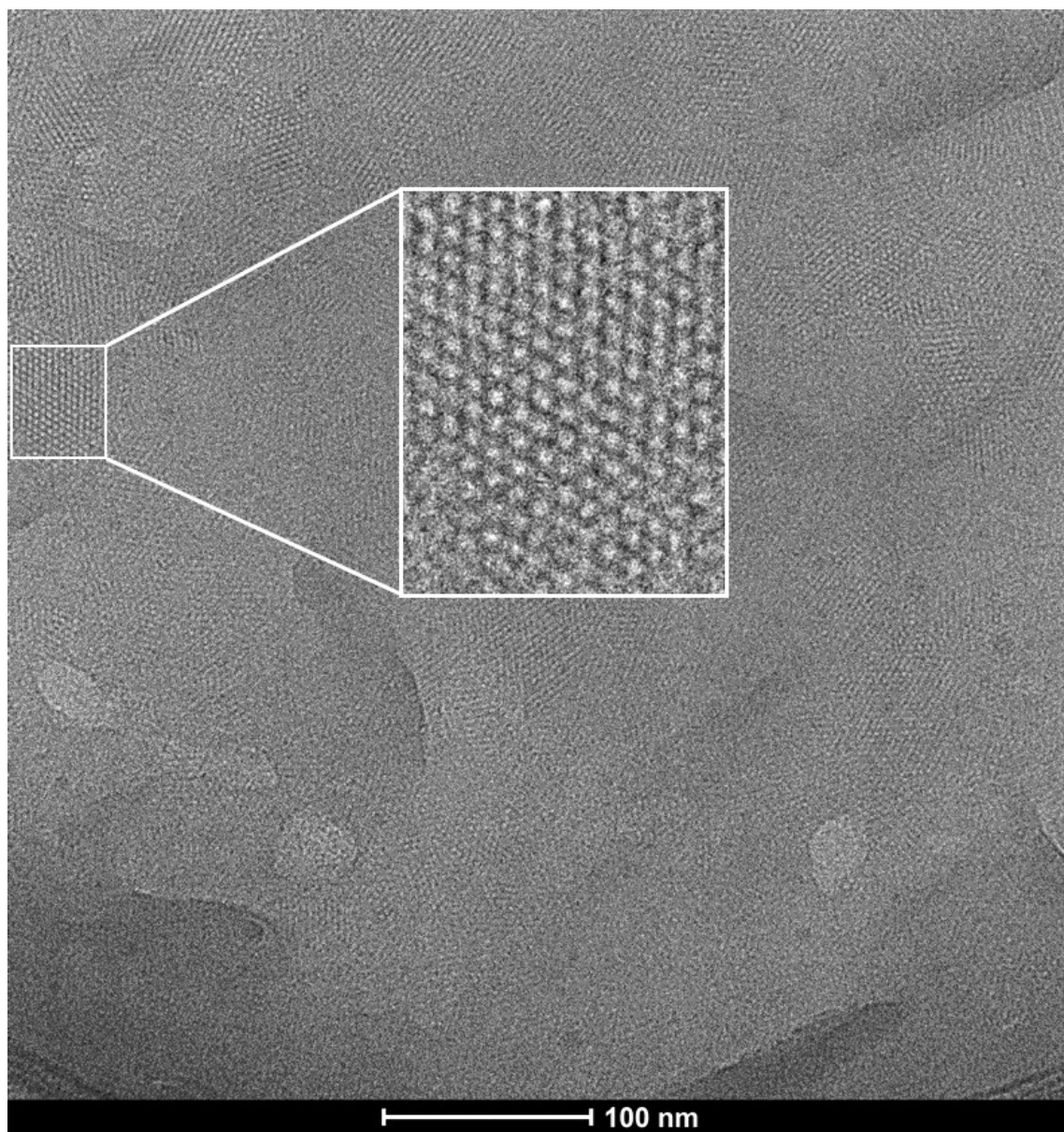


Figure S5. TEM of TAPB-PDA COF (LS) after 24 hours, 1 M acetic acid concentration.

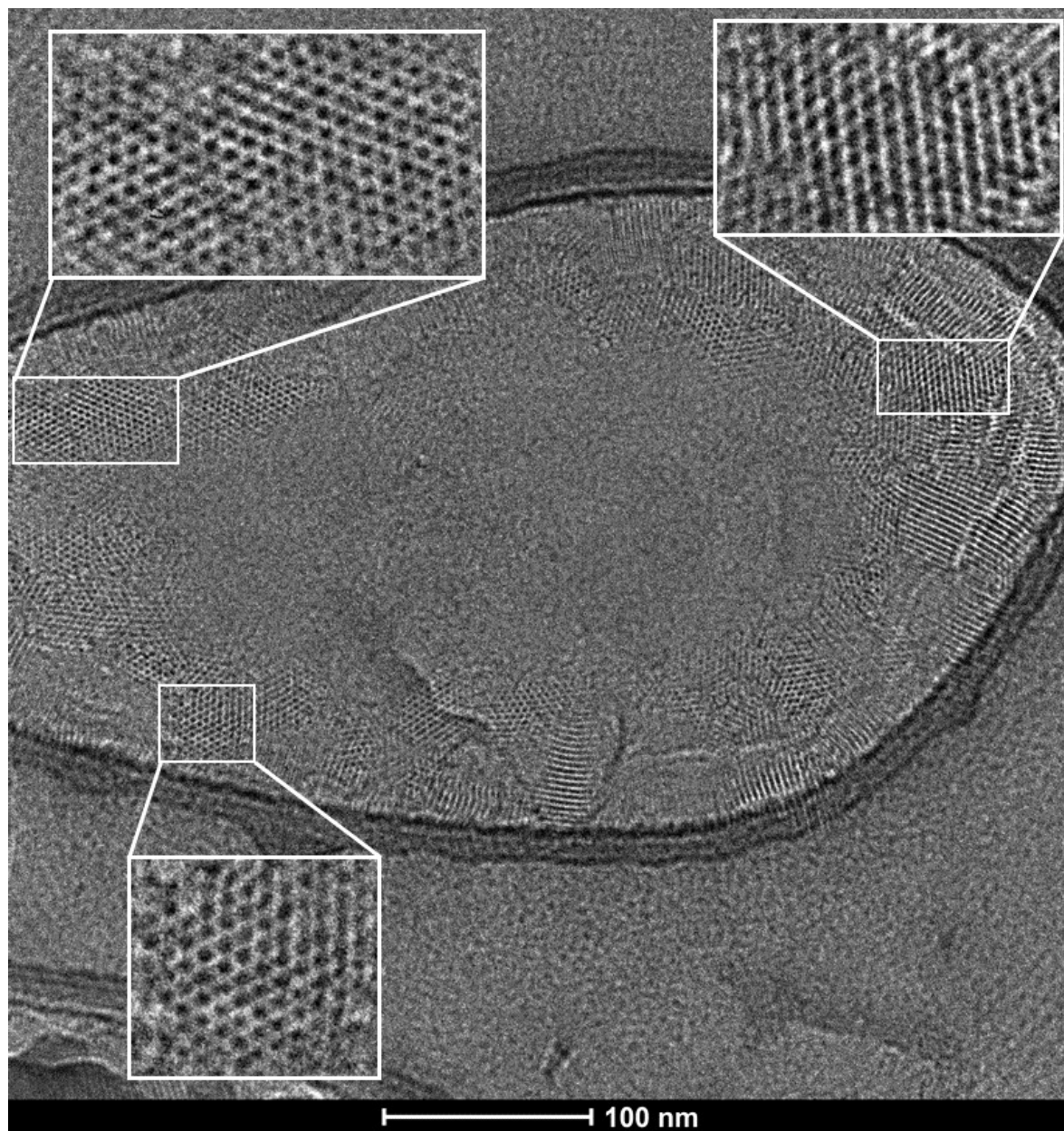


Figure S6. TEM of TAPB-PDA COF (LS) after 72 hours, 1 M acetic acid concentration.

Raman Spectroscopy of TAPB-PDA COF (LS) at Different Acid Concentrations

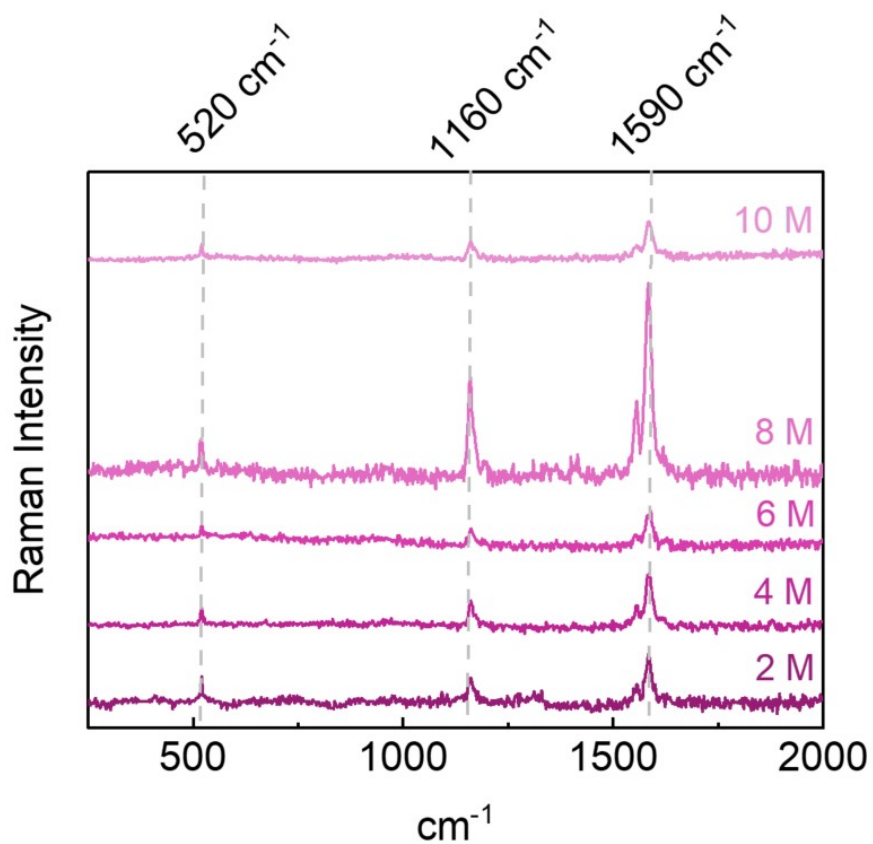


Figure S7. Raman spectra of TAPB-PDA COF (LS) on silicon grown at different acid concentrations (M), indicated in the bottom right. COF peaks correspond to 1660 cm^{-1} and 1590 cm^{-1} . Silicon substrate correspond to peak at 520 cm^{-1} .

Time-lapse of Interfacial COF Growth Setup

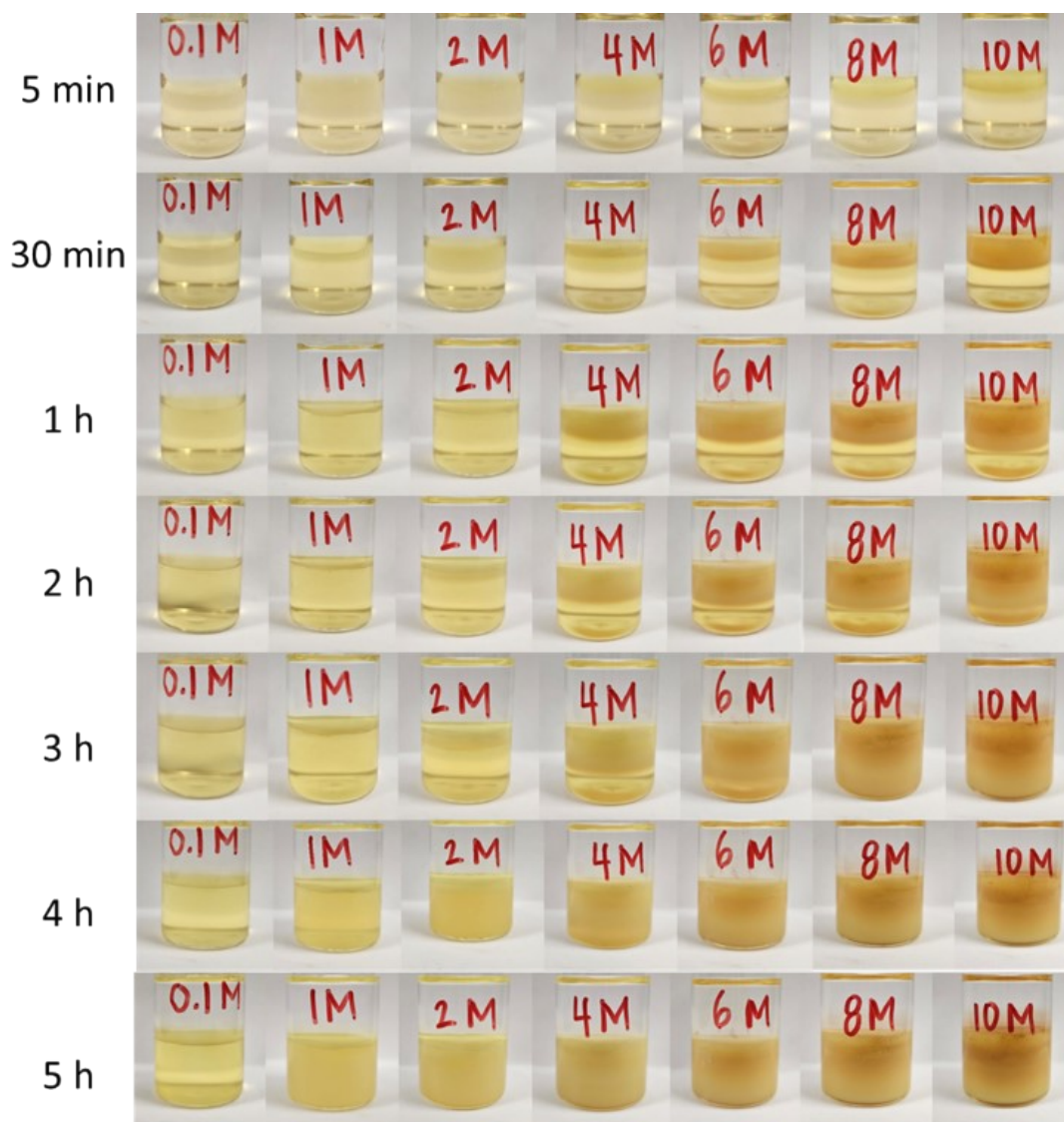


Figure S8. Time-lapse photographs of interfacial COF growth set up with 0.1 – 10 molar acetic acid concentration over 5 hours.

Film Morphology of TAPB-PDA COF (LS)

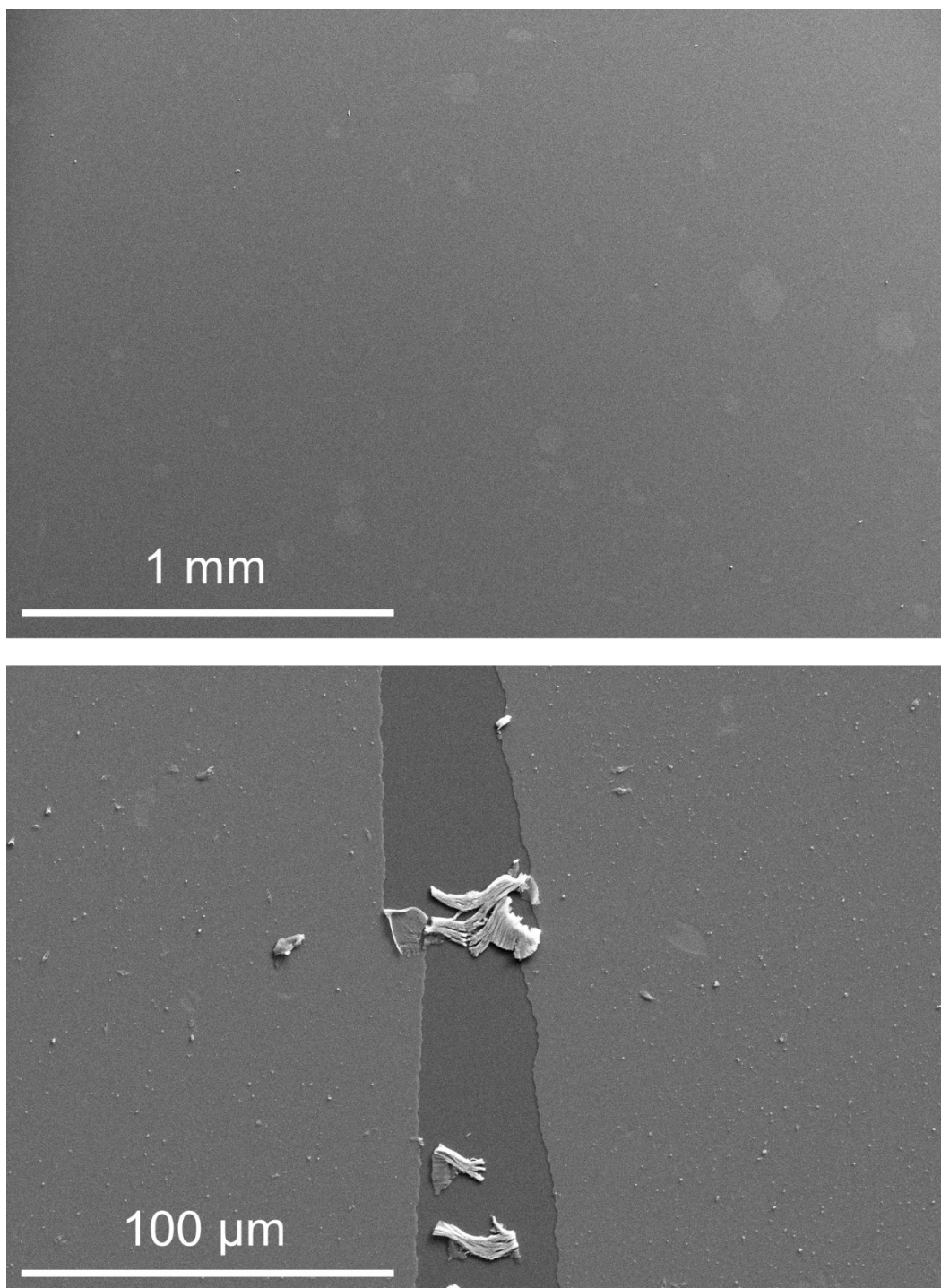


Figure S9. SEM Images of TAPB-PDA COF Film (LS) (2M, 24 hour growth).

Early Growth Experiment of TAPB-PDA COF (LS)

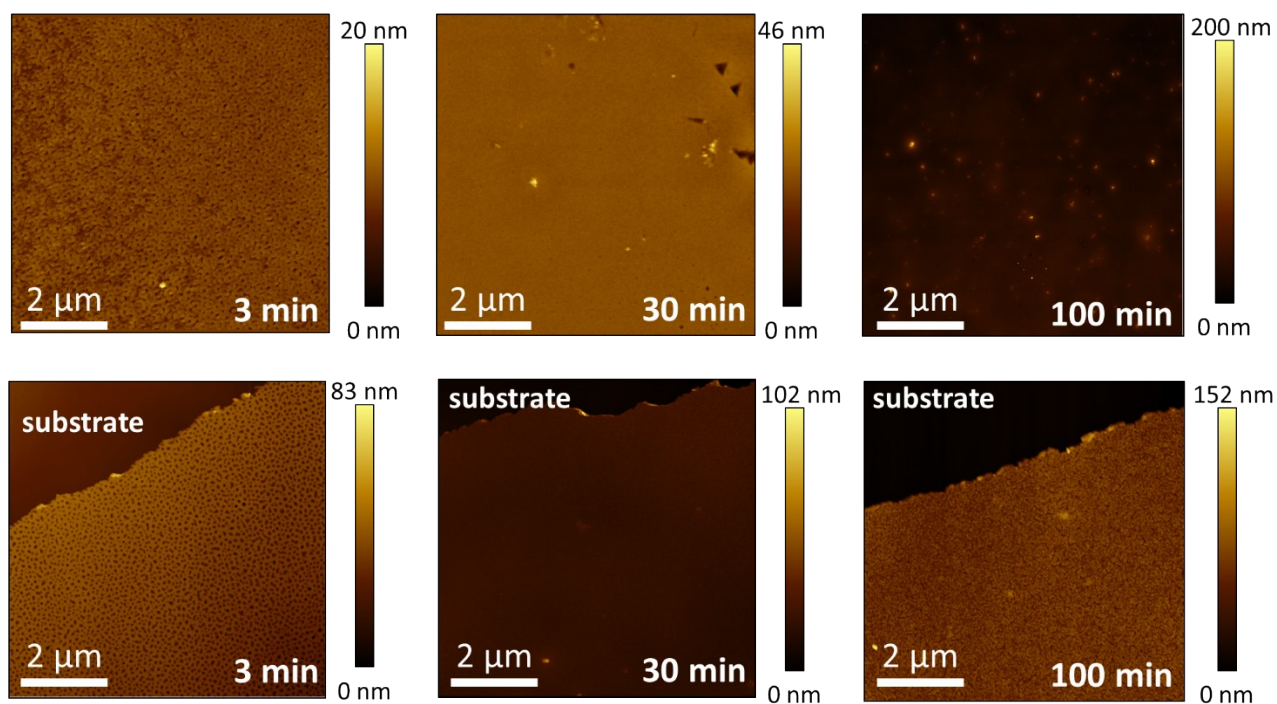


Figure S10. AFM image of LS film and edge growth in the first 100 minutes using 1 M acetic acid concentration.

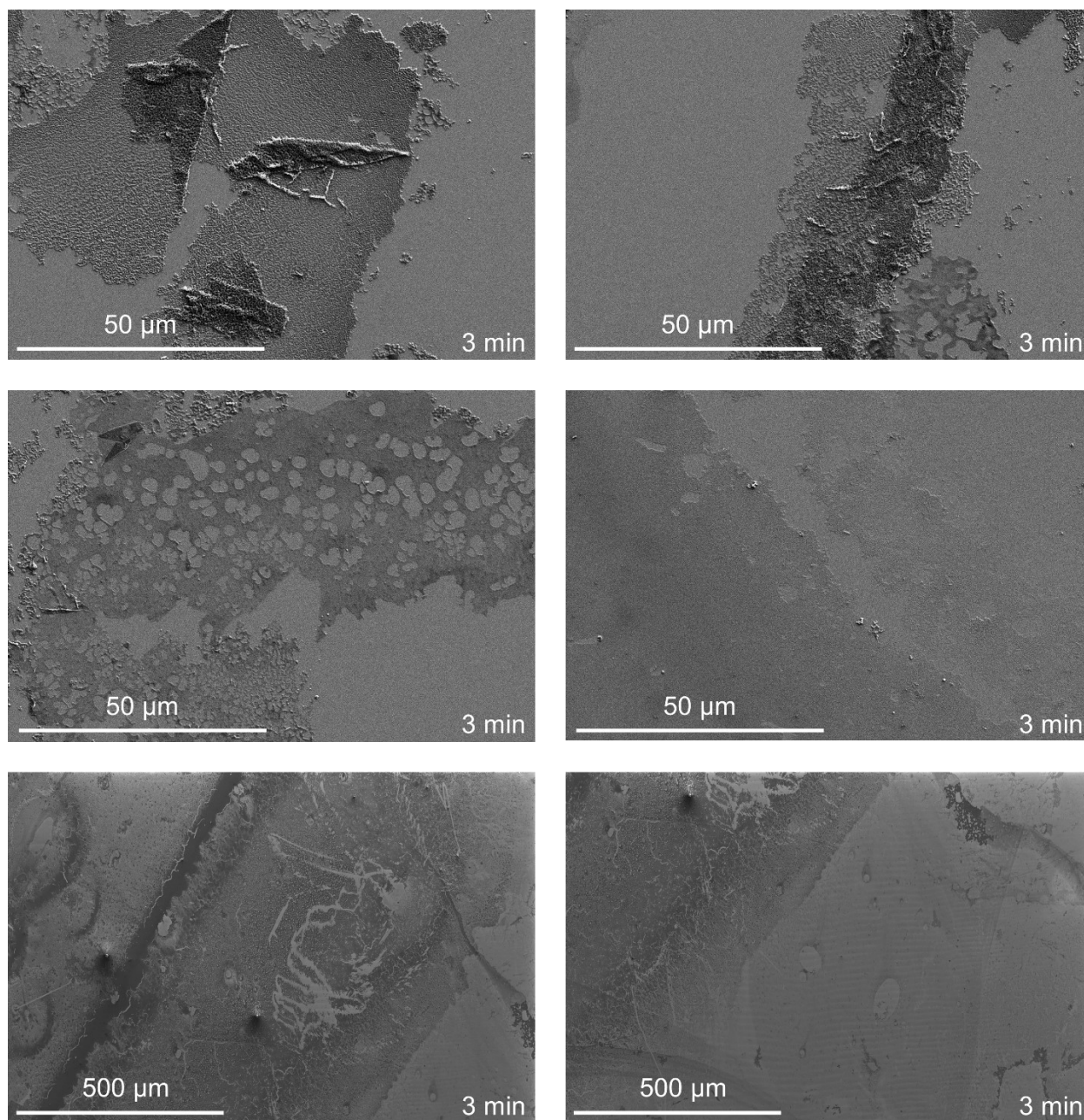


Figure S11. SEM image of LS film growth after 3 minutes using 1 M acid.

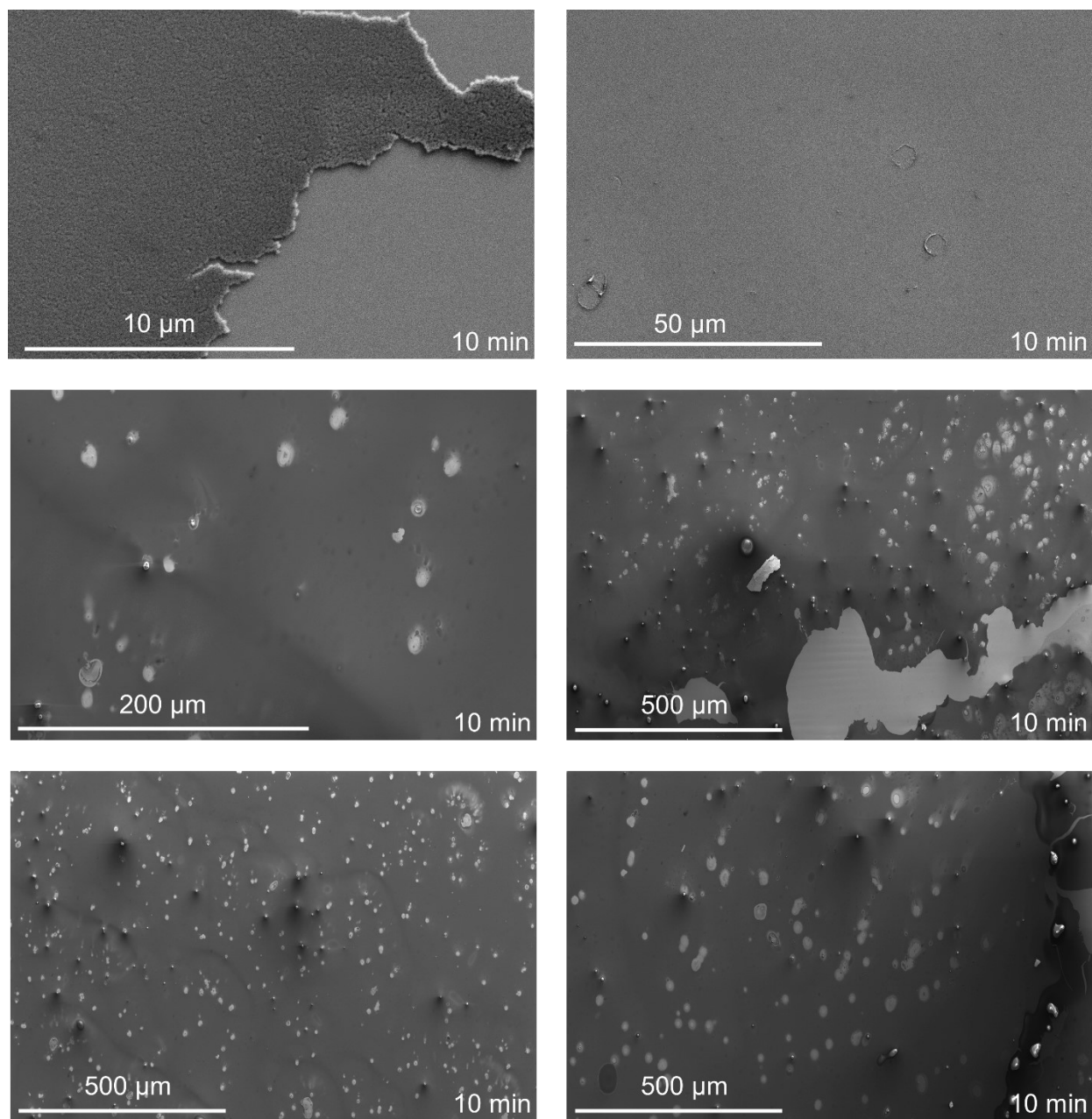


Figure S12. SEM image of LS film growth after 10 minutes using 1 M acid.

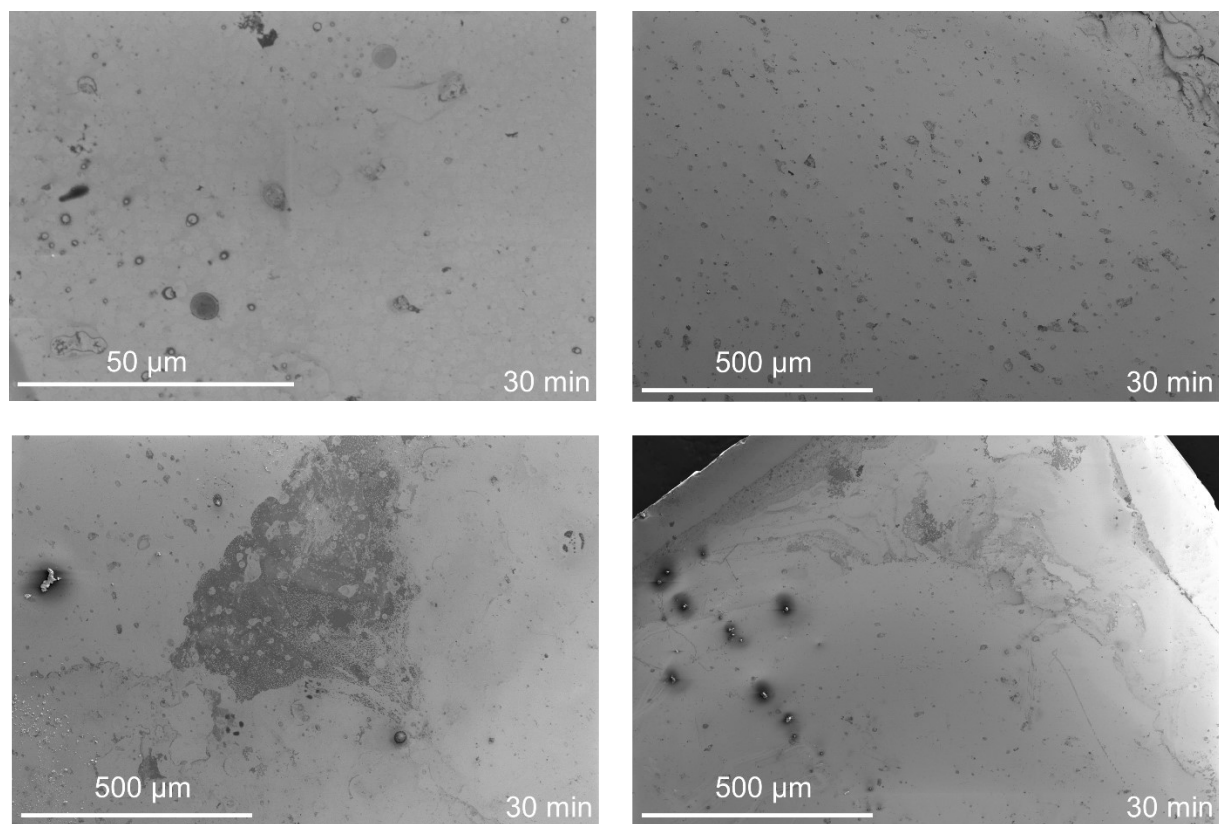


Figure S13. SEM image of LS film growth after 30 minutes using 1 M acid.

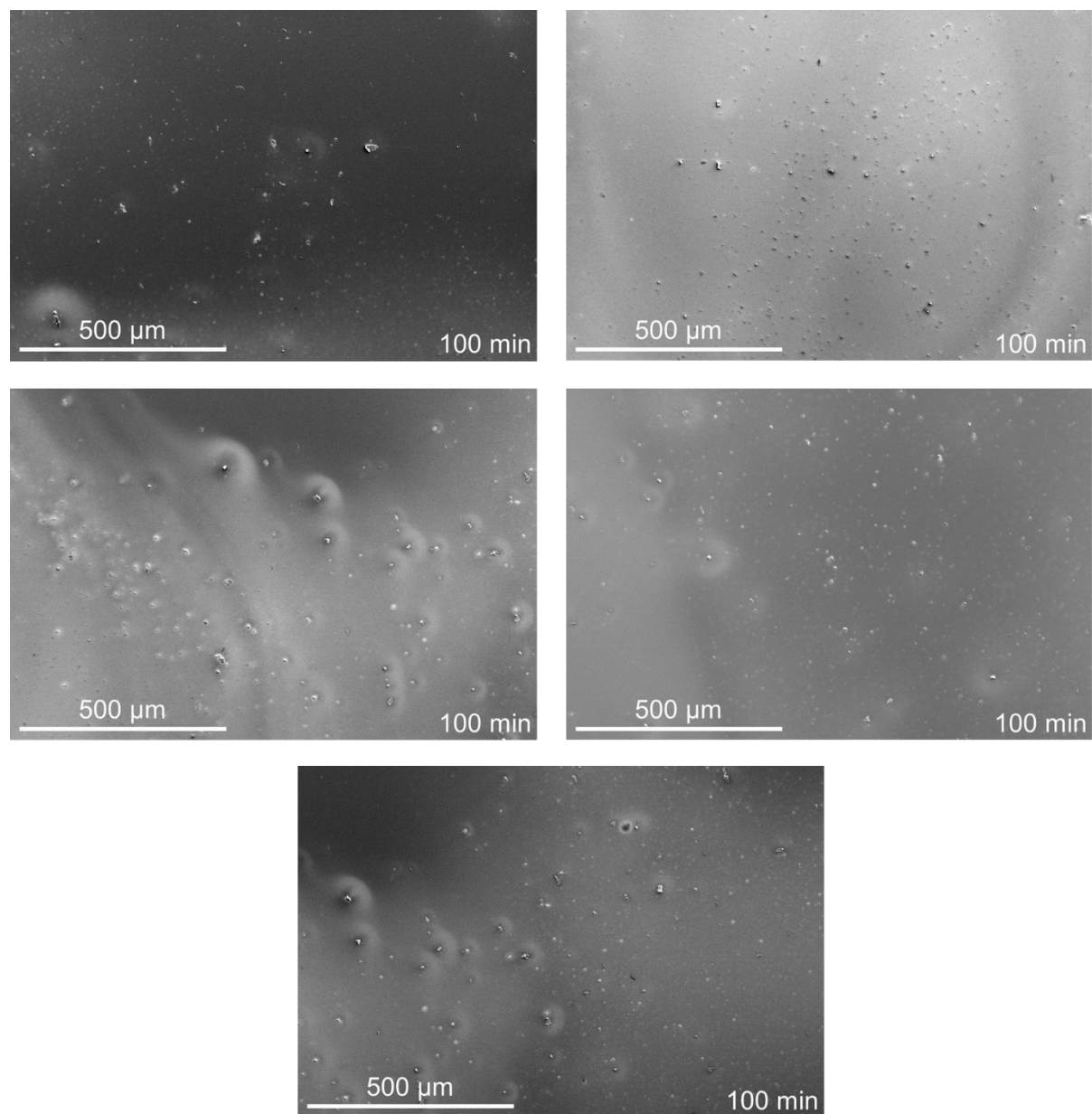


Figure S14. SEM image of LS film growth after 100 minutes using 1 M acid.

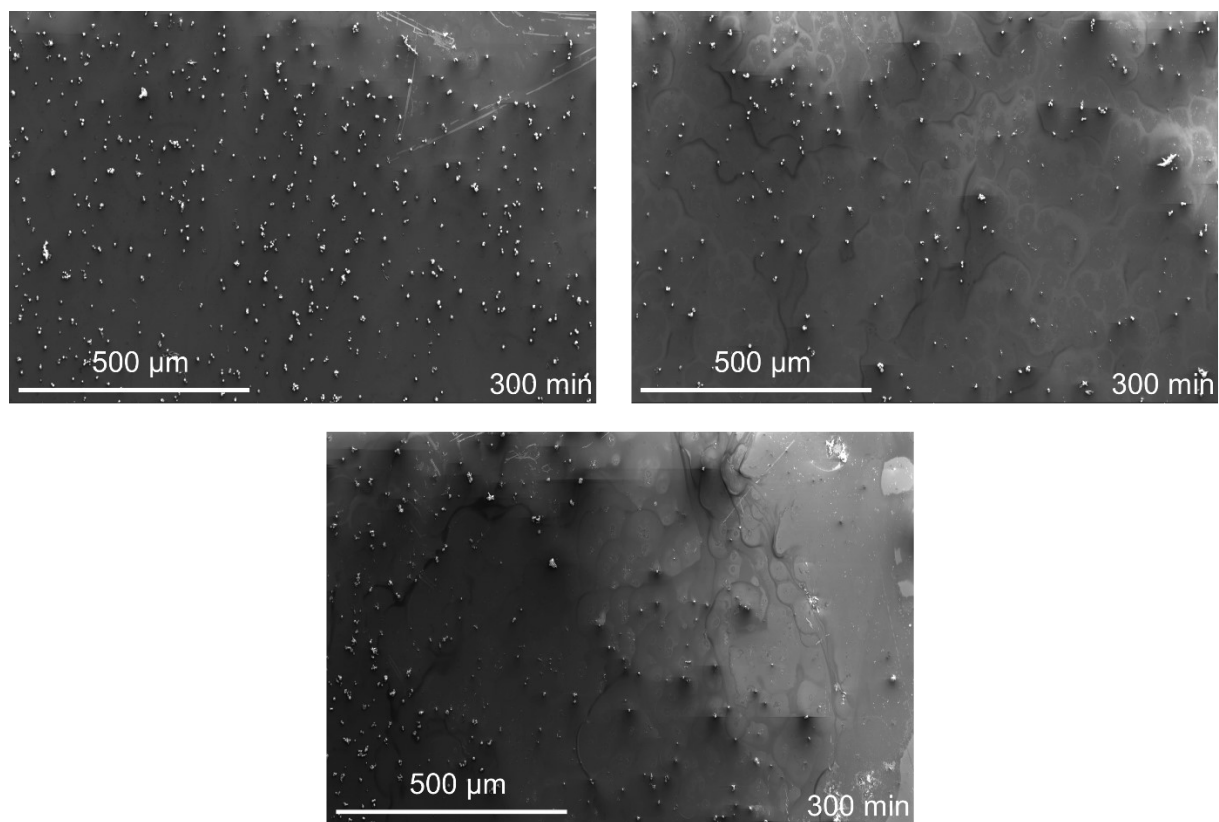


Figure S15. SEM image of LS film growth after 300 minutes using 1 M acid.

TAPB-PDA COF (LS) Regrowth Experiment

A regrowth experiment was performed to test if the thickness of the COF film could be increased by subjecting it to the same growth conditions again. Substrates were placed in growth setups under 1 M and 8 M conditions for 24 hours (1st growth). After being removed and sonicated, the film thickness was analyzed with AFM. Then part of the film was wiped away to expose the substrate (see top optical images in Figure S15). The substrates were then subjected to the same exact LS growth conditions for 24 hours again (2nd growth). The substrates were then analyzed with AFM again. A clear increase in thickness was observed where the 1st COF growth originally was. The side of the substrate containing the 1st growth & 2nd growth were twice as thick as the side containing just the 2nd growth.

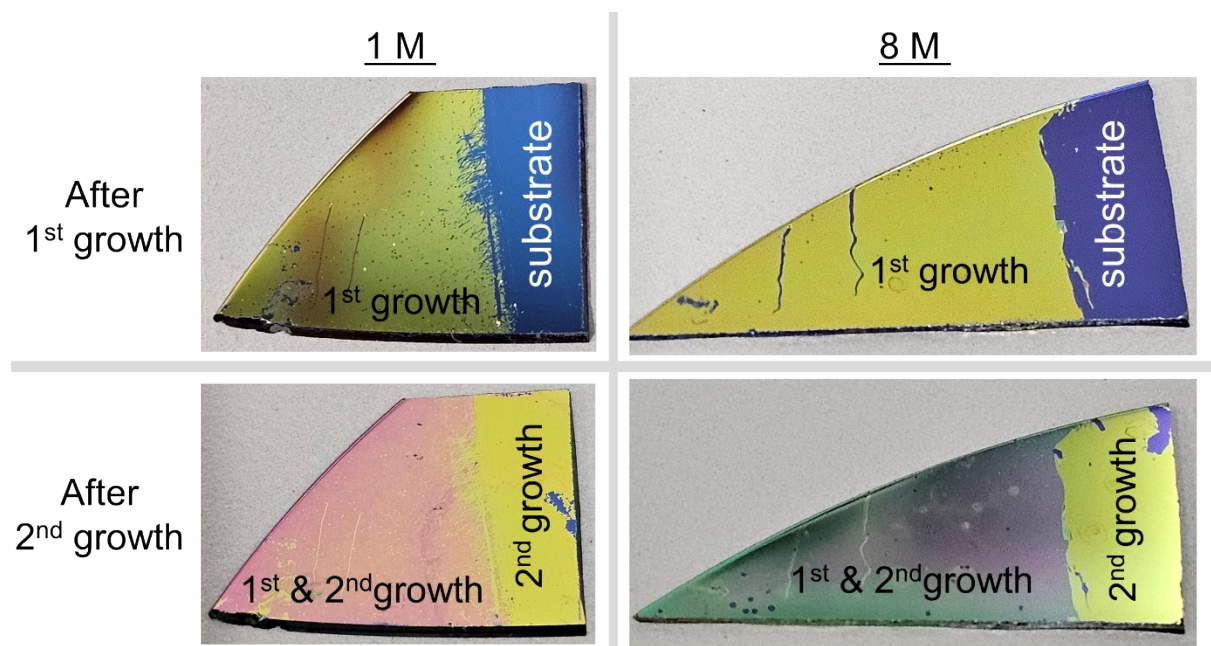


Figure S16. Optical Images of TAPB-PDA COF (LS) after first and second growth under 1 M and 8 M conditions

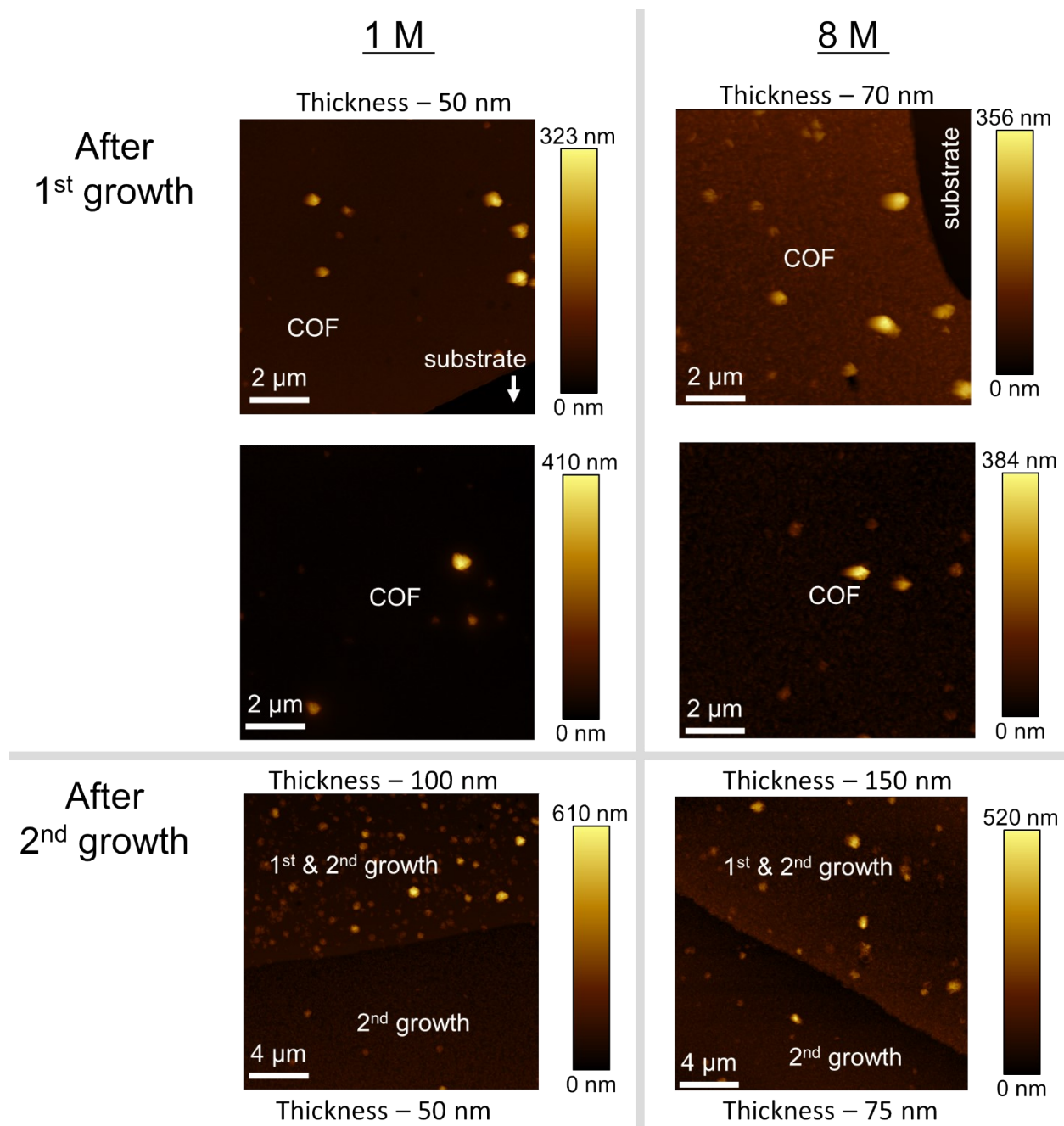


Figure S17. AFM Images of TAPB-PDA COF (LS) after first and second growth under 1 M and 8 M conditions

X-Ray Comparison of LL and LS TAPB-PDA COFs

Converting the PXRD pattern of the TAPB-PDA COF (LL) from 2θ to Q where λ is the wavelength of the Cu K- α 1.54 Å^{5,6}:

$$Q = \frac{4\pi}{\lambda} \sin\left(\frac{2\theta}{2}\right)$$

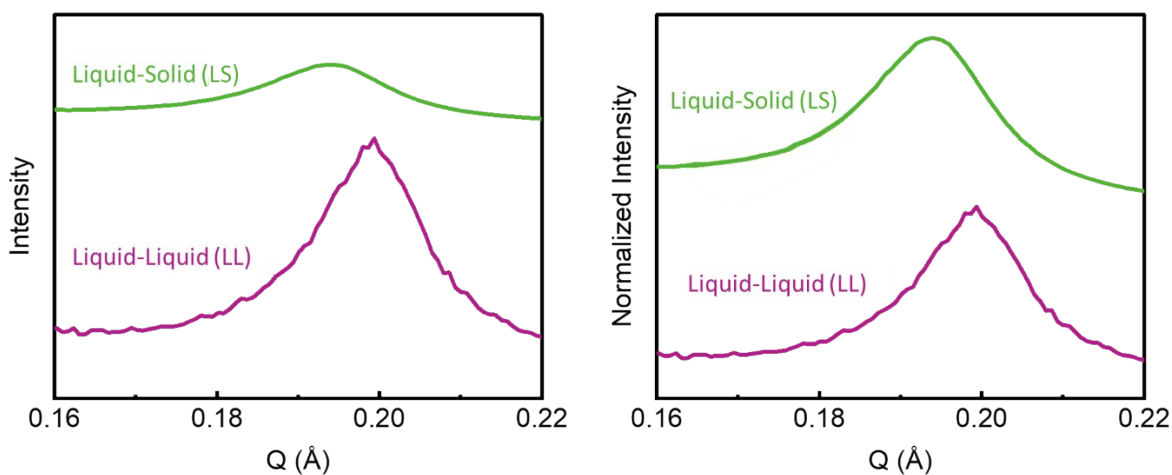


Figure. S18 Comparison of LL and LS TAPB-PDA COF in terms of Q (Å⁻¹)

PXRD pattern of liquid–liquid COF (purple) after converting to Q and 1D GIWAXS projection of liquid–solid (COF/LS2). A close alignment of peaks can be observed in the same Q range. The Q value for the [100] peak of the hexagonal lattice of the TAPB-PDA COFs appears at 0.195 Å⁻¹ for the LS film and 0.2 Å⁻¹ for the LL film indicating a d-spacing of 32 Å and 31 Å, respectively.

Lattice Constant Calculation of LS and LL TAPB-PDA COF from GIWAXS

The lattice constant, a , was also calculated for the three samples shown in Figure 6a-d using the following equation:

$$d_{Bragg} = \frac{a}{\sqrt{\frac{4}{3}(h^2 + k^2 + hk) + \frac{a^2}{c^2}l^2}}$$

The lattice constants are 37.2 Å, 37.4 Å, 37.2 Å, and 38.3 Å, respectively, which also match previous literature report for the same COF.⁷

V. Device Information

Fabrication

The fabrication process of the transistor is shown in Fig. S1. First nLOF 2035 photoresist (negative) was spin-coated onto a pre-cleaned Si/300 nm SiO₂ wafer at 3500 rpm and baked at 110°C for 1 minute. The substrates were then exposed to UV light using a mask aligner instrument (Suss MABA6) and developed using AZ 300K for 45 seconds before a post backing process at 110°C for 1 minute. Then 5 nm of Cr and 100 nm of Au (rate: 0.5 ~ 2.0 Å/s) were thermally evaporated and placed for overnight liftoff in acetone to obtain source and drain electrode. Two layers of Parlyene-C (2µm for each layer) were coated onto the substrates with an anti-adhesive layer (Micro-90) between them using a SCS Labcoter 2. The first layer acts as an encapsulation layer while the second layer acts as a sacrificial layer for COF patterning. To further pattern the channel area, SU-8 photoresist was spin-coated at 3000rpm and baked at 95°C for 3 minutes. The substrates were then exposed to UV light using a mask aligner instrument (Suss MABA6) and post-backed at 95°C for 5 minutes then developed in SU-8 developer for 1 minute. Parlyene-C was etched from the channel and contact area using an RIE (SAMCO) at 160 W with 10 sccm of CHF₃ and 50 sccm of O₂ for 25 minutes. The COF film was then grown onto the substrate in-situ using the liquid–solid growth methods described above. The device was then subjected to the same annealing and activation steps described on page S4. Following this, sacrificial Parylene-C was peeled-off of the layer to pattern the channel material.

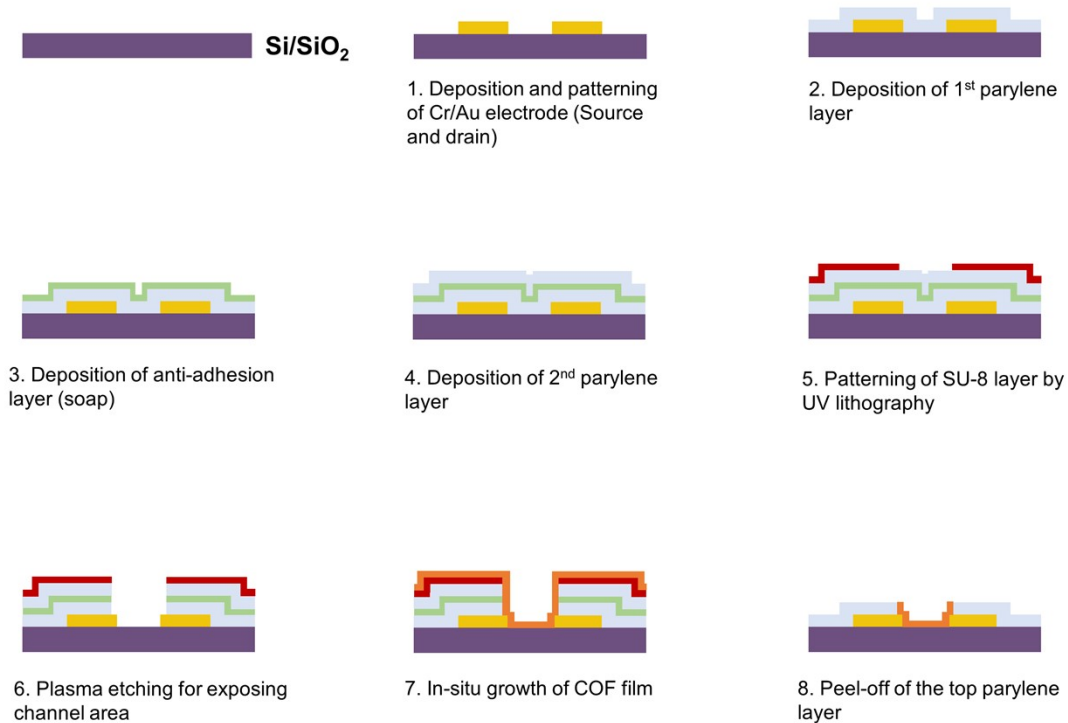


Figure S19. Fabrication process flow of COF-based transistor device.

Transistor Measurement

Electrical characterization of the COF-based OECTs was carried with an Agilent B1500A semiconductor parameter analyzer in ambient. A droplet of PBS (1×) was applied on the channel area, and a separated Ag/AgCl electrode was inserted in the droplet acting as the gate electrode. The voltage sweeping speed was 0.1 V/s, and all measurements were carried out in ambient.

VI. References

- 1) S. Stoupin, T. Krawczyk, D. Sagan, A. Temnykh, L. Smieska, A. Woll, J. Ruff, A. Lyndaker, A. Pauling, B.P. Croom, E.B. Trigg, Side-bounce beamlines using single-reflection diamond monochromators at Cornell High Energy Synchrotron Source, *J. Synchrotron Rad.* **28** (2021), 429–438.
- 2) Schneider, C. A.; Rasband, W. S.; Eliceiri, K. W. NIH Image to ImageJ: 25 years of image analysis. *Nature Methods*, **9** (7), 671-675.
- 3) L. D. Tran, B. J. Ree, A. Ruditskiy, L. K. Beagle, R. C. Selhorst, D. D. Bhagwandin, P. Miesle, L. F. Drummy, M. F. Durstock, R. Rao, H. Koerner, N. R. Glavin and L. A. Baldwin, .
- 4) S. A. Ahmed, Q. Liao, Q. Shen, M. M. F. Ashraf Baig, J. Zhou, C. Shi, P. Muhammad, S. Hanif, K. Xi, X. Xia and K. Wang, *Chemistry A European J*, 2020, **26**, 12996–13001.
- 5) J. L. Baker, L. H. Jimison, S. Mannsfeld, S. Volkman, S. Yin, V. Subramanian, A. Salleo, A. P. Alivisatos and M. F. Toney, *Langmuir*, 2010, **26**, 9146–9151.
- 6) J. W. Colson, A. R. Woll, A. Mukherjee, M. P. Levendorf, E. L. Spitler, V. B. Shields, M. G. Spencer, J. Park and W. R. Dichtel, *Science*, 2011, **332**, 228–231.
- 7) Li, Rebecca L.; Yang, A.; Flanders, N. C.; Yueng, M. T.; Sheppard, D. T.; Dichtel, W. R.; Two Dimensional Covalent Organic Framework Solid Solutions, *J. Am. Chem. Soc.*, 2021, **143**, 7081-7087.